Examination of production and properties of $^{268-271}$Hs

G. G. Adamian,[1] N. V. Antonenko,[1,2] L. A. Malov,[1] and H. Lenske[3]
[1]*Joint Institute for Nuclear Research, RU-141980 Dubna, Russia*
[2]*Mathematical Physics Department, Tomsk Polythechnic University, 634050 Tomsk, Russia*
[3]*Institut für Theoretische Physik der Justus-Liebig-Universität, D-35392 Giessen, Germany*
(Received 18 July 2017; published 9 October 2017)

The production cross sections of several isotopes of Hs and their properties are considered. The optimal reactions are predicted for producing $^{268-271}$Hs. The possible α-decay chains including these isotopes are analyzed and compared with the available experimental data. The number of new isomeric states is predicted in the nuclei of these α-decay chains. The role of α decay in the identification of these isomeric states is discussed.

DOI: 10.1103/PhysRevC.96.044310

I. INTRODUCTION

Heavy-ion fusion reactions have been extensively used to produce superheavy nuclei and to extend the number of their isotopes [1,2]. The ratio between the cross sections in different fusion-evaporation channels is important for the correct identification of each isotope by α-decay or spontaneous fission. In addition to ^{269}Hs studied in the α-decay chains of ^{273}Ds [3] and ^{277}Rg [4], the isotopes ^{270,271}Hs have been investigated [5,6]. The interesting result was the observation of the $3n$ evaporation channel in the ^{26}Mg + ^{248}Cm reaction at energies just below the Coulomb barrier. The calculation of the evaporation residue cross sections in $(2-5)n$ evaporation channels of strongly asymmetric reactions demands the accurate treatment of the capture probability in the entrance channel because the collision occurs at energies near the Coulomb barrier and the effect of the mutual orientation of deformed colliding nuclei should be taken into account. Note that a large set of Hs isotopes can be obtained just in these reactions with valuable cross sections.

The stability of heavy nuclei is governed by nuclear shell structure whose influence is dramatically amplified near closed proton and neutron shells [3]. The ^{270}Hs has been predicted to be a doubly magic deformed nucleus [7–9]. The direct experimental evidence for the new subshell closures at $Z = 108$ and $N = 162$ was first provided by the α-decay properties of the nuclei ^{262}Rf, ^{265,266}Sg, ^{267}Hs, and ^{273}Ds [3]. In Ref. [5], the doubly magic ^{270}Hs has been observed based on a rapid chemical isolation.

The study of Hs isotopes is of interest because they are less deformed than the neighboring nuclei and the neutron subshell at $N = 162$ is the most pronounced there. The Hs isotopes considered can be produced directly in fusion-evaporation channel as well as in the α-decay chain of a heavier nucleus. A comparison of the decays of differently produced Hs isotope could reveal the isomeric states and structure peculiarities. The potential energy surface near the ground state could have some shallow minima which affect the ground-state wave function. So, the role of these minima in the α-decay chain is of interest.

In the present paper we consider the properties of $^{268-271}$Hs produced in the reactions ^{22}Ne + ^{249}Cf, ^{26}Mg + ^{248}Cm, ^{30}Si + ^{244}Pu, ^{36}S + ^{238}U, and ^{48}Ca + ^{226}Ra (Sec. II). The effects of the deformation and mutual orientation of colliding nuclei is taken into account to calculate the capture cross sections at energies near the Coulomb barrier. The properties and α-decay chains containing these isotopes of Hs are studied within the microscopic-macroscopic approach (Sec. III). The K- and shape-isomeric states are found and discussed in the nuclei of these α-decay chains (Secs. III C and III D). Finally, we summarize our results in Sec. IV.

II. EVAPORATION RESIDUES

The production of Hs isotopes is estimated with the dinuclear system (DNS) model [10–24] in which the fusion-evaporation proceeds in three steps which affect the evaporation residue cross section in the xn evaporation channel

$$\sigma_{\rm ER}^{xn}(E_{\rm c.m.}) = \sum_{J=0} \sigma_{\rm fus}(E_{\rm c.m.},J) W_{\rm sur}^{xn}(E_{\rm c.m.},J),$$
$$\sigma_{\rm fus}(E_{\rm c.m.},J) = \int_0^{\pi/2}\int_0^{\pi/2} d\cos\Theta_1 d\cos\Theta_2\, \sigma_c \times (E_{\rm c.m.},J,\Theta_i) P_{\rm CN}(E_{\rm c.m.},J,\Theta_i). \quad (1)$$

Here, we introduce the averaging over the orientations of statically deformed interacting nuclei [Θ_i ($i = 1,2$) are the orientation angles with respect to the collision axis]. The quadrupole deformation parameters of actinides are taken from Ref. [25]. With Eq. (1) one can consider the collision of deformed nuclei at energies near the Coulomb barrier which is a function of Θ_i. One can also calculate the compound nucleus formation at sub-barrier energies. In the first step of a fusion reaction the projectile is captured by the target. The value of $\sigma_c(E_{\rm c.m.},J,\Theta_i)$ defines the transition of the colliding nuclei over the Coulomb barrier and the formation of the DNS when the kinetic energy $E_{\rm c.m.}$ and angular momentum J of the relative motion are transformed into the excitation energy and angular momentum of the DNS. In the second step a formed DNS evolves into the compound nucleus in the mass asymmetry coordinate [10–13,16]. In Eq. (1), $P_{\rm CN}$ is the probability of compound nucleus formation after the capture. Since the bombarding energy $E_{\rm c.m.}$ of the projectile is usually higher than the Q value for fusion, the produced compound nucleus is excited. In the third step of the reaction

TABLE I. The evaporation residue cross sections $\sigma_{\rm ER}^{xn}(th.)$ calculated at the maxima of excitation function of xn channels in the indicated reactions leading to Hs isotopes. The excitation energies $E_{\rm CN}^{*}$ of compound nuclei are listed. The mass table of Ref. [34] is used in the calculations. The experimental cross sections $\sigma_{\rm ER}^{xn}$(exp) are from Refs. [6,35,36].

Reaction	$E_{\rm CN}^{*}$ (MeV)	xn	$\sigma_{\rm ER}^{xn}(th.)$ (pb)	$\sigma_{\rm ER}^{xn}$(exp) (pb)	Hs isotope
^{22}Ne + ^{249}Cf	35.2	3n	1.5		^{268}Hs
	46	4n	3.4		^{267}Hs
^{26}Mg + ^{248}Cm	33.4	3n	1.5	∼2.5 [6]	^{271}Hs
	44.8	4n	10	∼3 [6]	^{270}Hs
	50.8	5n	6	∼7 [6]	^{269}Hs
^{30}Si + ^{244}Pu	33.4	3n	0.7		^{271}Hs
	46	4n	5.1		^{270}Hs
	51.4	5n	4.4		^{269}Hs
^{36}S + ^{238}U	34.6	3n	0.5	<2.9 [35]	^{271}Hs
	43.6	4n	4	$0.8^{+2.6}_{-0.7}$ [35]	^{270}Hs
	49.6	5n	1.1	<1.5 [35]	^{269}Hs
^{48}Ca + ^{226}Ra	32.8	3n	7.2		^{271}Hs
	38.8	4n	7	16^{+13}_{-7} [36]	^{270}Hs

the compound nucleus loses its excitation energy mainly by the emission of particles and γ quanta [26–33]. The survival probability $W_{\rm sur}^{xn}$ of the excited compound nucleus in the xn evaporation channel takes into account the de-excitation of the compound nucleus formed. The fission barrier $B_f = B_f^{\rm LD} + B_f^{M}$ of compound nucleus has a liquid drop part $B_f^{\rm LD}$ and a microscopical part B_f^{M}. For the considered heavy isotopes of Hs, $B_f^{\rm LD} = 0.2$ MeV. The value $B_f^{M} = \delta W_{\rm sd}^{A} - \delta W_{\rm g.s.}^{A}$ is the difference between the shell correction $\delta W_{\rm g.s.}^{A}$ of the nucleus with mass number A at the ground state [34] and the shell correction $\delta W_{\rm sd}^{A}$ at the saddle point. Usually one can set $\delta W_{\rm sd}^{A} = 0$. The variation of $\delta W_{\rm sd}^{A}$ from 0 to 1 MeV leads to a variation of the maxima of excitation functions of about factor of 2. The details of calculation of $\sigma_{\rm fus}$ as well as $W_{\rm sur}^{xn}$ are presented in Ref. [22] where the excitation functions for number of reactions are shown. Because we are interested in the production of $^{268–271}$Hs, in Table I we only list the evaporation residue cross sections for these isotopes in the maxima of corresponding excitation functions.

As shown in Ref. [22], at energies just below the Coulomb barrier the evaporation residue cross section does not drop fast because the loss in fusion cross section is compensated by the gain of survival probability. To produce directly the isotopes ^{268}Hs, ^{269,270}Hs, and ^{271}Hs with the largest cross sections, one can use the reactions ^{22}Ne + ^{249}Cf, ^{26}Mg + ^{248}Cm, and ^{48}Ca + ^{226}Ra, respectively. The calculated values of $\sigma_{\rm ER}^{xn}$ ($x = 3, 4, 5$) in the ^{26}Mg + ^{248}Cm reaction are compared in Ref. [22] with the experimental data [6]. The theoretical and experimental excitation functions are in a good agreement within the experimental and theoretical uncertainties. So, the DNS model is able to describe and predict the evaporation residue cross sections in strongly asymmetric reactions at energies near the barriers.

III. STRUCTURE OF NUCLEI NEAR HS

A. Microscopic-macroscopic approach

In order to study the structure of a nucleus near its ground state, one can use, for example, the models of Refs. [7–9,34,37–43] based on various shape parametrizations. The proper shape parametrization allows us to reduce the number of collective variables and to simplify the microscopic treatment. In the present paper we choose the shape parametrization adopted in the two-center shell model [42]. With this simple parametrization one can easily trace the evolution of a nucleus from the ground state to the separate fission fragments. In the two-center shell model the nuclear shapes are defined by the following set of coordinates. The elongation $\lambda = l/(2R_0)$ measures the length l of the system in units of the diameter $2R_0$ of the spherical compound nucleus. For large elongations, this variable starts to describe the relative motion of fission fragments. The transition of the nucleons through the neck is described by the mass asymmetry η. The neck parameter $\varepsilon = E_0/E'$ is defined by the ratio of the actual barrier height E_0 to the barrier height E' of the two-center oscillator. The deformations $\beta_i = a_i/b_i$ of axial symmetric fragments are defined by the ratio of their semiaxes. In the compact shapes β_i are related only to the left and right sides of the nucleus along the symmetry axis.

For the compact nuclear shapes near the ground state, one can set $\varepsilon = 0$ and $\eta = 0$. Therefore, we have only three parameters: λ, β_1, and β_2 to describe the deformations of various multipolarities. The octupole deformation occurs in the case of $\beta_1 \neq \beta_2$. The case of $\beta_1 = \beta_2 = \beta$, which is treated here, means the absence of the static deformations of odd multipolarities. One can show that the quadrupole deformation parameter β_{02} strongly depends on the value of λ while the hexadecapole deformation parameter β_{04} is mostly sensitive to the value of β. For ^{248}Fm, in Fig. 1 the dependencies of β_{02} and β_{04} on λ and β are shown. With given values of λ and β the quadrupole and hexadecapole moments are firstly calculated. Then the values of β_{02} and β_{04}, which correspond to these moments, are found. The ground state of ^{248}Fm is found at $\lambda_{\rm g.s.} = 1.18$ and $\beta_{\rm g.s.} = 1.28$ that corresponds to $\beta_{02} = 0.25$ and $\beta_{04} = 0.027$. The ground state of ^{270}Hs is found at $\lambda_{\rm g.s.} = 1.14$ and $\beta_{\rm g.s.} = 1.06$ that corresponds to $\beta_{02} = 0.25$ and $\beta_{04} = -0.03$. In Ref. [34], $\beta_{02} = 0.231$ and $\beta_{04} = -0.086$ are predicted for this nucleus. The examples of nuclear shapes produced by the two-center shell model have been presented in Ref. [44]. In the framework of macroscopic-microscopic model [43] the quadrupole deformation of ^{270}Hs is $\beta_{02} = 0.26$.

With the two-center shell model the potential energy near the ground state can be calculated as the sum of two terms

$$U(\lambda,\beta) = U_{\rm LDM}(\lambda,\beta) + \delta U_{\rm mic}(\lambda,\beta). \quad (2)$$

The first term is a smoothly varying macroscopic energy calculated with the liquid drop model. The second term $\delta U_{\rm mic}$ contains the shell and pairing corrections arising due to the shell structure of the nuclear system. The absolute values

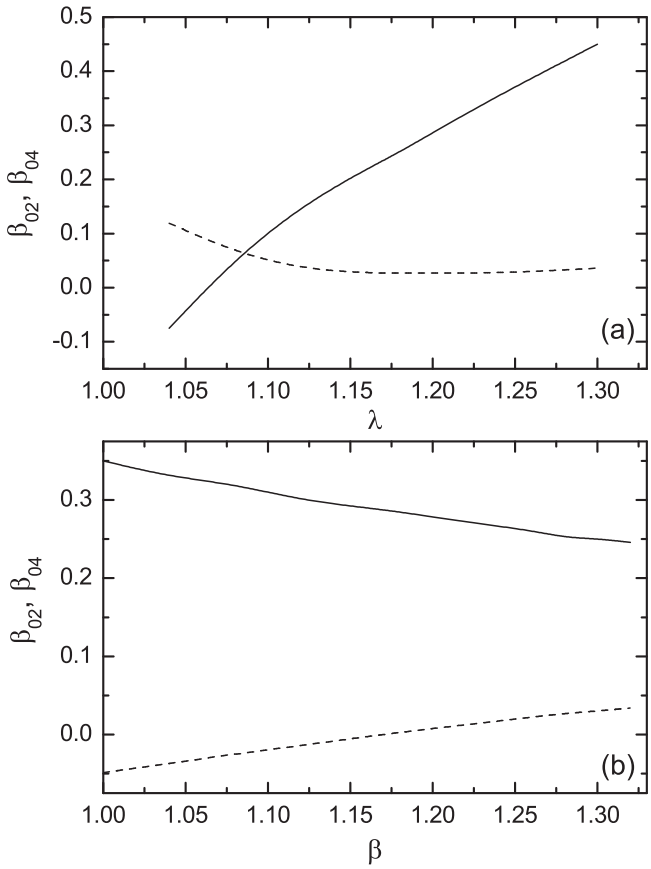

FIG. 1. The calculated dependencies of quadrupole (β_{02}, solid lines) and hexadecapole (β_{04}, dashed lines) deformation parameters on λ (a) at $\beta = 1.28$ and on β (b) at $\lambda = 1.18$ for ^{248}Fm.

of microscopic corrections obtained in our calculations for the ground states seem to be close to those obtained in Refs. [34,37] for nuclei with $Z \leqslant 112$ [45]. In the nuclei considered the position $(\lambda_{\text{g.s.}}, \beta_{\text{g.s.}})$ of the ground state is defined by minimizing $U(\lambda, \beta)$.

The contribution of an odd nucleon, occupying a single-particle state $|\mu\rangle$ with energy e_μ, to energy of a nucleus is described by the one-quasiparticle energy $\sqrt{(e_\mu - e_F)^2 + \Delta^2}$. Here, the Fermi energy e_F and the pairing-energy gap parameter Δ are calculated with the BCS approximation in accordance with the procedure of Ref. [39]. Pairing interaction of the monopole type with strength parameters $G_{\substack{n \\ p}} = (19.2 \mp 7.4\frac{N-Z}{A})A^{-1}$ MeV [39] for neutrons and protons is used. The used values of G_n and G_p are comparable with those in Refs. [37,40]. To take it effectively into account in the calculations of one-quasiparticle excitations $E_\mu = \sqrt{(e_\mu - e_F)^2 + \Delta^2} - \sqrt{(e'_\mu - e_F)^2 + \Delta^2}$ and two-quasiparticle excitations $E_\mu = \sqrt{(e_\mu - e_F)^2 + \Delta^2} + \sqrt{(e'_\mu - e_F)^2 + \Delta^2}$, where e'_μ is the single-particle energy of occupied level below the Fermi level energies, we use the results of Ref. [40] where the reduction of Δ by about factor of 0.85 occurs. For comparison, the values of Δ obtained by us agree with those in Refs. [34,37] within 0.1 MeV.

The momentum-dependent part of the single-particle Hamiltonian of the two-center shell model consists of the spin-orbit and l^2-like terms (see Ref. [42]) with the parameters $\kappa_{n,p}$ and $\mu_{n,p}$, respectively. As known, these parameters depend on the nuclear mass number A and influence the quantum numbers of the last occupied single-particle level. In order to improve the description of the low-lying one-quasiparticle states in well-studied heavy nuclei, in Refs. [44,45] we introduced the weak dependence on $(N - Z)$ in the parameters $\kappa_{n,p}$ and $\mu_{n,p}$. Indeed, in the calculations with Woods-Saxon single-particle potential the dependence on $(N - Z)$ is included into the momentum-independent part of the potential. Here, with the Nilsson-type single-particle potential the weak dependence on $(N - Z)$ is incorporated into the momentum-dependent part of the single-particle Hamiltonian. With obtained values of $\kappa_{n,p}$ and $\mu_{n,p}$ we are able to describe correctly the ground-state spins of many heavy nuclei treated.

The binding energies $B(Z,A)$ of nuclei in the ground states are calculated in accordance with Ref. [45]. Here, these energies are used to calculate only the $Q_\alpha(Z,A)$ values for the α-decays from the ground-state-to-ground-state. As shown in Ref. [45], the calculated values of Q_α are in a good agreement (within 0.3 MeV) with the most of available experimental values of Q_α.

In order to estimate α-decay half-lives T_α, we use the expression recently suggested in Ref. [46]:

$$\log_{10} T_\alpha(Z,A) = 1.5372Z(Q_\alpha - E_\mu)^{-1/2} - 0.1607Z - 36.573, \quad (3)$$

where E_μ is the excitation energy of quasiparticle state to which the α-decay occurs.

B. Verification of calculations of one- and two-quasiparticle spectra

In the deformed mean field, the single-particle and one-quasiparticle states with the projection $K = \Lambda \pm 1/2$ of total angular momentum and parity π are marked as $K^\pi|Nn_z\Lambda>$, where N (the shell quantum number), n_z (the number of the quanta along the z axis), and Λ (the projection of orbital angular momentum) are the asymptotic quantum numbers [39].

To demonstrate the quality of the description of the experimental one-quasiparticle spectra, we show in Fig. 2 the quasiparticle spectrum for ^{245}Pu. One can see that the discrepancy in energy with experimental values [47] does not exceed 300 keV that is quite satisfactory. Since the octupole correlations are absent in our model, some negative parity states can have lower energies.

In Fig. 3, the calculated energies of one-quasiparticle as well as rotational states of ^{249}Fm are in good agreement with the experimental data [48]. The energies of the rotational states $9/2^+$ and $11/2^+$ are calculated as in Ref. [49]. The characteristics of the α decay of ^{253}No are well described as well.

In Ref. [44], we demonstrated a good description of the energies of two-quasiparticle states with $K^\pi = 8^-_\nu$ [the index ν (π) denotes neutron (proton) pair] in the isotones from ^{176}Yb till ^{184}Pt as well as in the even isotopes of No. With

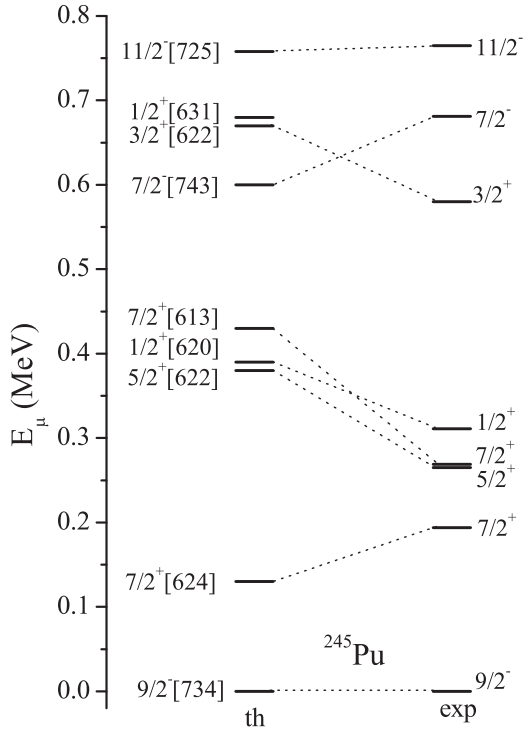

FIG. 2. The calculated (th) and experimental (exp) [47] energies E_μ (in MeV) of one-quasiparticle states in ^{245}Pu.

our approach one can describe well the isotonic and isotopic trends in energy of one- and two-quasiparticle states. In lighter nuclei, for example ^{158}Gd, the calculated energies of two-quasiparticle states $4^+_\pi[5/2^+[413] \otimes 3/2^+[411]]$ and $4^-_\nu[3/2^-[521] \otimes 5/2^+[642]]$ are 1.44 and 1.48 MeV, respec-

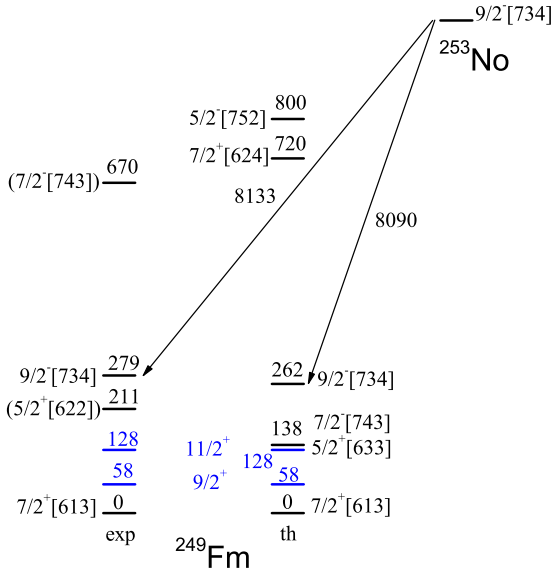

FIG. 3. The calculated (th) and experimental (exp) [48] energies (in keV) of one-quasiparticle states in ^{249}Fm. The rotational states $9/2^+$ and $11/2^+$ build on the ground state are shown as well. The calculated value of $Q_\alpha = 8.09$ MeV for ^{253}No is compared with the experimental $Q^{\rm exp}_\alpha = 8.133$ MeV.

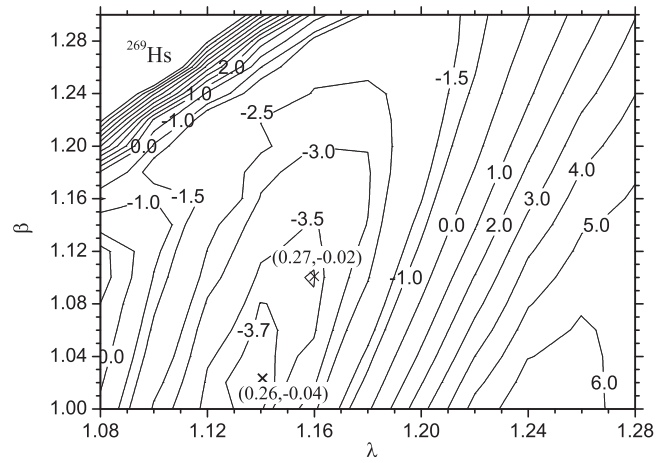

FIG. 4. The calculated potential energy surface of ^{269}Hs as a function of λ and β. The potential energy is with respect to the liquid-drop part at $\lambda = 1$ and $\beta = 1$. The potential energy minima are marked by crosses. The solid cross corresponds to the ground state potential minimum. The numbers in brackets near the crosses denote the parameters of quadrupole (β_{02}) and hexadecapole (β_{04}) deformations.

tively, that is in a good agreement with the experimental values [47], 1.38 and 1.636 MeV, for $K^\pi = 4^+$ and 4^- states, respectively. Thus, the model seems to be verified in the region of well-studied nuclei and can be applied to predict the spectra for heavier nuclei.

C. Potential energy surfaces and shape isomeric states at normal deformations

Besides the shape-isomer minimum, if exists, at large deformation, inside of the internal fission barrier of heavy nucleus there is usually one (ground state) potential minimum on the potential energy surface as a function of deformation parameters. However, in some nuclei the potential energy surface as a function of deformation parameters is more complicated and can have several minima due to the shell effects [50,51]. The deepest one, where the shell correction is maximum, is related to the ground state. The role of other shallow minima (the shape isomers) in the vicinity of the ground state is not well pronounced. With the shape parametrization used here the potential energy surface is well unfolded near the ground state to allow the additional potential minima to be notable. The potential energy surfaces of ^{269,270}Hs, ^{265,266}Sg, and ^{261}Rf with indication of all minima are presented in Figs. 4–8. Besides the ground state potential minima, there are additional potential minima in the nuclei ^{269}Hs ($11/2^-_1$ at 0.135 MeV), ^{270}Hs (0^+_1 at 0.22 MeV and 0^+_2 at 1.4 MeV), ^{265}Sg ($1/2^-_1$ at 0.56 MeV), ^{266}Sg (0^+_1 at 0.14 MeV and 0^+_2 at 0.26 MeV), and ^{261}Rf ($3/2^+_1$ at 0.034 MeV and $3/2^+_2$ at 0.28 MeV). In contrast, there is only the ground-state potential minimum in ^{262}Rf. The spins of the nuclei in these minima are the same like in the corresponding ground states. As follows from our calculations, the additional minima in the region of heavy nuclei exist only in some nuclei with $104 \leqslant Z \leqslant 108$. They appear in the region where the

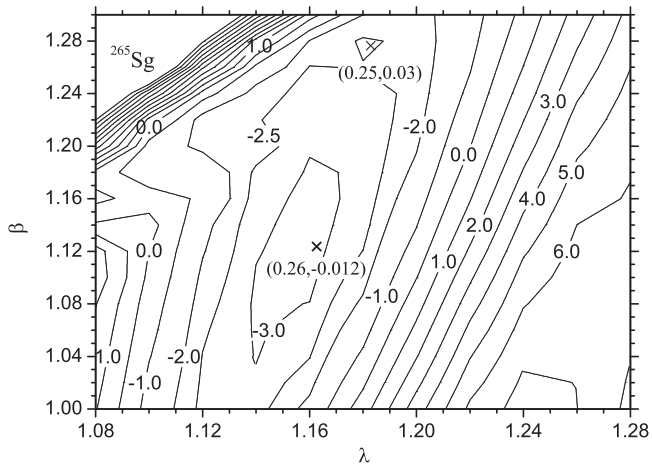

FIG. 5. The same as in Fig. 4, but for ^{265}Sg.

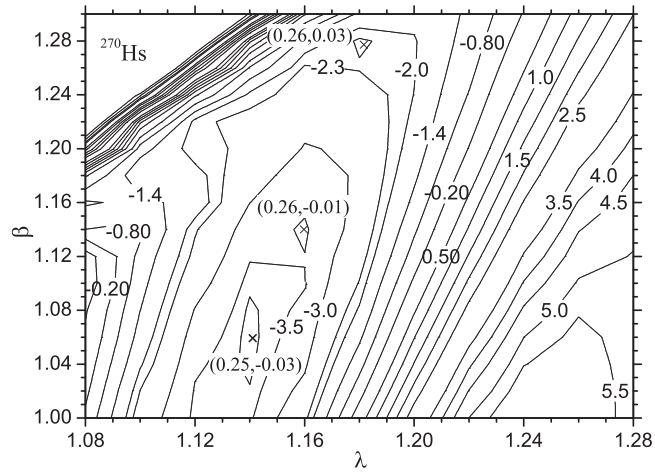

FIG. 7. The same as in Fig. 4, but for ^{270}Hs.

potential energy surface is rather flat and correspond to almost the same quadrupole deformation parameters and different hexadecapole deformation parameters. Note that the rather strong increase of pairing strength, by about 50%, washes out the additional potential minima.

To demonstrate the sensitivity of the potential energy surface to the single-particle potential used to calculate the microscopic part $\delta U_{\rm mic}$ in Eq. (2), we present in Fig. 9 the results obtained with the Woods-Saxon single-particle spectrum [53,54]. So, in the calculations with Eq. (2), the two-center oscillator single-particle spectrum is replaced by that of the Woods-Saxon potential. As seen, the position of the ground-state minimum almost remains at the same β_{02} and β_{04}. One additional potential minimum 0^+_1 is also pronounced. It appears at almost the same quadrupole deformation, but at other hexadecapole deformation than that in Fig. 7. So, the appearance of additional minima is the general feature of the microscopic-macroscopic method applied to the region of Hs isotopes. However, the number and position of these minima in β_{04} depend on the single-particle potential used. If there will some experimental evidences for the additional potential minima in the α-decay chains, one can perhaps estimate the hexadecapole deformation in the region of the heavies nuclei.

The available experimental data are not sufficient to conclude whether the found shallow potential minima, the shape-isomers at the normal deformations, really exist. Also, the experimental confirmation will be a nontrivial task. The nucleus will not stay long enough in these minima to observe the γ transitions. However, the α decay of the parent nucleus can populate the states located in the minima closed in energy to the ground-state minimum. Therefore, the presence of additional potential minima in the daughter nucleus would lead to some variation of the observed energies of α particles for the parent nucleus. For example, the lowest additional potential minimum at 0.034 MeV in ^{261}Rf is expected to play a role in the α decay of ^{265}Sg.

D. Quasiparticle spectra, K, and shape isomers

1. α-decay chain containing ^{269}Hs

The one-quasiparticle spectra build on the ground state are presented in Fig. 10 for the nuclei of the α-decay chain

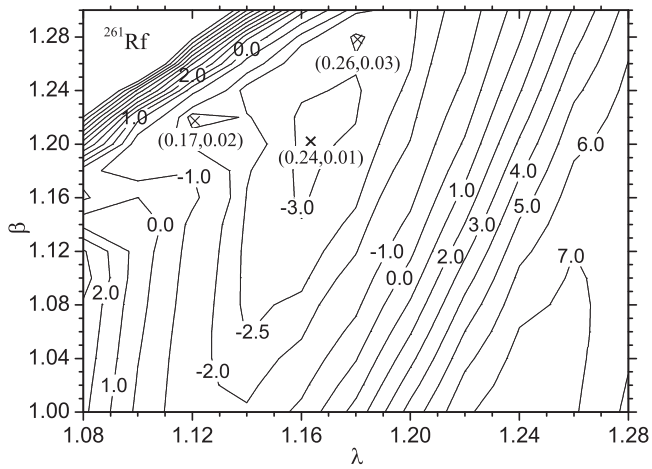

FIG. 6. The same as in Fig. 4, but for ^{261}Rf.

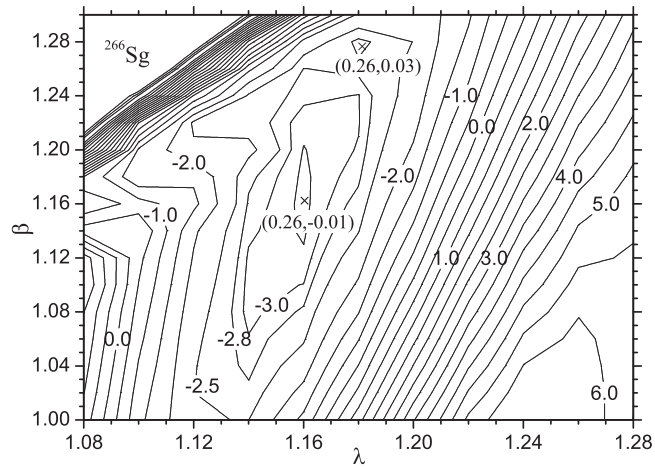

FIG. 8. The same as in Fig. 4, but for ^{266}Sg.

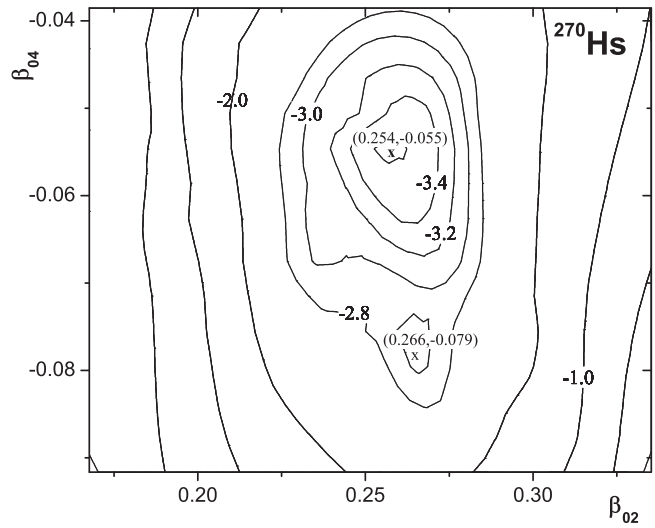

FIG. 9. The potential energy surface of ^{270}Hs as a function of β_{02} and β_{04} obtained with the Woods-Saxon single-particle spectrum used to calculate $\delta U_{\rm mic}$. The potential energy is with respect to the liquid-drop part of spherical nucleus. The potential energy minima are marked by crosses. The solid cross corresponds to the ground state potential minimum. The numbers in brackets near the crosses denote the parameters of quadrupole (β_{02}) and hexadecapole (β_{04}) deformations.

^{269}Hs $\rightarrow$ ^{265}Sg $\rightarrow$ ^{261}Rf $\rightarrow$ ^{257}No. The calculated values of Q_α for the ground-state-to-ground-state α decays are indicated. The most probable α decays are shown in Fig. 10 and listed in Table II. The calculated energies of α decays are in satisfactory agreement with the available experimental data [4–6,52,55] (see Table II). The α decay of the ground state of ^{265}Sg can occur as follows: ^{265}Sg$(1/2^-) \rightarrow$ ^{261}Rf$(1/2^-_1)$ with $Q_\alpha = 8.69$ MeV that is more preferable than the transition ^{265}Sg$(1/2^-) \rightarrow$ ^{261}Rf$(1/2^-)$ with $Q_\alpha = 8.59$ MeV because the state $1/2^-_1[761]$ is lower in energy than the state $1/2^-[761]$. In ^{261}Rf, the $E2$ transition between $3/2^+_1$ and ground state would need about 30 s because of the small energy difference and influence of pairing correlations. For the α decays ^{261}Rf$(3/2^+) \rightarrow$ ^{257}No$(3/2^+)$, ^{261}Rf$(7/2^+) \rightarrow$ ^{257}No$(7/2^+)$, and ^{261}Rf$(1/2^-_1) \rightarrow$ ^{257}No$(1/2^-)$ the values of $Q_\alpha = 8.54$, 8.62, and 8.49 MeV agree well with the experimental values of $Q_\alpha = 8.41$ and 8.65 MeV [4–6,52,55]. Since in ^{261}Rf the $E1$ transition between $1/2^-_1[761]$ and $3/2^+_1[622]$ (or $3/2^+[622]$) is strongly suppressed, one can not exclude the α decay from the possible isomer state $1/2^-_1$. Moreover, from this state the nucleus ^{261}Rf can decay by spontaneous fission due to the small hindrance in K.

As seen in Fig. 10, there are K-isomeric states $1/2^-[761]$, $7/2^+[613]$, $7/2^+[613]$, and $1/2^+[620]$ in ^{269}Hs, ^{265}Sg, ^{261}Rf, and ^{257}No, respectively. While in our calculations $7/2^+[613]$ is the ground state of ^{257}No, in Ref. [56] the $3/2^+[622]$ was assigned to the ground state. However, at the energies of γ transitions measured in Ref. [56] the internal conversion coefficients do not allow us the firm discrimination between $M1$ and $E2$ transitions. In addition, the states $7/2^+[613]$ and $3/2^+[622]$ are close in energy in our calculation.

In Fig. 11, the one-quasiparticle spectra of the ground states are presented for the nuclei ^{253}Fm, ^{273}Ds, and ^{277}Cn which together with the nuclei shown in Fig. 10 belong to the α-decay chain of ^{277}Cn. The ground-state potential minima in ^{277}Cn and ^{273}Ds correspond to $\beta_{02} = 0.21$, $\beta_{04} = -0.05$, and $\beta_{02} = 0.25$, $\beta_{04} = -0.02$, respectively. Because of the change of the deformation parameters, particular β_{04}, the levels $9/2^+[604]$ and $9/2^+[615]$ have different order in ^{277}Cn and ^{273}Ds. In ^{277}Cn and ^{273}Ds the isomeric states are $9/2^+[604]$ and $1/2^-[761]$, respectively, because the α decays from these states occur faster than the γ transitions estimated. Since in ^{277}Cn the $M2$ transition between $13/2^-[716]$ and $9/2^+[604]$ needs about 2.3 ms as follows from the Wiesskopf estimate, the state $13/2^-[716]$ can be treated as the isomer because the α decay from it is faster time, about 1.1 ms. The possible

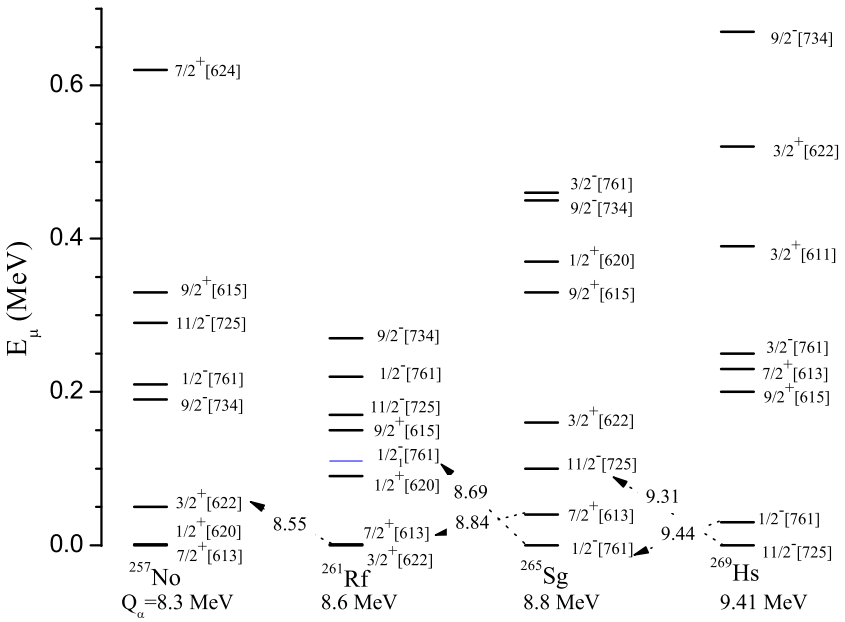

FIG. 10. The calculated spectra of one-quasineutron states in the indicated nuclei. For the ground-state-to-ground-state α decays, the calculated values of Q_α are listed. Possible α decays are shown by arrows with corresponding values of Q_α.

TABLE II. Possible α decays of indicated heavy nuclei starting from ^{277}Cn. The calculated values of Q_α and T_α, and tentatively related experimental values $Q_\alpha^{\rm exp}$ of Q_α are listed.

Nucleus	Decay mode	Q_α (MeV)	T_α	$Q_\alpha^{\rm exp}$ (MeV)
^{277}Cn	$1/2^-[761] \xrightarrow{\alpha} 1/2^-[761]$	11.575	100 μs	11.62 [4], 11.49 [55]
	$9/2^+[604] \xrightarrow{\alpha} 9/2^+[604] \xrightarrow{\gamma's} 9/2^+[615]$	11.254	560 μs	11.33 [4], 11.25 [55]
	$13/2^-[716] \xrightarrow{\alpha} 13/2^-[716] \xrightarrow{\gamma's} 9/2^+[615]$	11.12	1100 μs	
^{273}Ds	$9/2^+[615] \xrightarrow{\alpha} 9/2^+[615] \xrightarrow{\gamma's} 11/2^-[725]$	11.08	340 μs	11.25 [4] 10.73, 10.88, 11.01 [3]
	$1/2^-[761] \xrightarrow{\alpha} 1/2^-[761]$	11.265	130 μs	11.37 [4], 11.31, 11.32 [55]
^{269}Hs	$11/2^-[725] \xrightarrow{\alpha} 11/2^-[725] \xrightarrow{\gamma} 7/2^+[613]$	9.31	3.03 s	9.09, 9.27 [6], 9.31 [55]
	$1/2^-[761] \xrightarrow{\alpha} 1/2^-[761]$	9.44	1.28 s	9.32, 9.37 [4], 9.39 [55]
^{265}Sg	$1/2^-[761] \xrightarrow{\alpha} 1/2^-_1[761] \xrightarrow{\gamma} 3/2^+[622]$	8.686	48 s	8.75 [4], 8.64, 8.76 [3]
	$7/2^+[613] \xrightarrow{\alpha} 7/2^+[613]$	8.84	15.7 s	8.82 [6], 8.84 [3,55]
^{261}Rf	$3/2^+[622] \xrightarrow{\alpha} 3/2^+[622] \xrightarrow{\gamma} 7/2^+[613]$	8.54	26.3 s	8.41 [6,55], 8.33 [3]
	$7/2^+[613] \xrightarrow{\alpha} 7/2^+[613]$	8.62	17 s	8.64 [6], 8.65 [4]
^{257}No	$7/2^+[613] \xrightarrow{\alpha} 7/2^+[613]$	8.23	49 s	8.35 [52]
	$1/2^+[620] \xrightarrow{\alpha} 1/2^+[620]$	8.3	29 s	8.47 [4], 8.45 [52], 8.42 [3]

α decays of ^{273}Ds and ^{277}Cn are tentatively related to the available experimental data [3,4,6,52,55] in Table II.

2. α-decay chain containing ^{271}Hs

In the nuclei of possible α-decay chain ^{271}Hs $\rightarrow$ ^{267}Sg $\rightarrow$ ^{263}Rf $\rightarrow$ ^{259}No, the additional shallow potential minima exist in ^{271}Hs ($11/2^-_1$ at 1.33 MeV), ^{267}Sg ($11/2^-_1$ at 0.1 MeV and $9/2^+_2$ at 0.8 MeV), and ^{263}Rf ($1/2^-_1$ at 0.17 MeV) (Figs. 12–14). However, the α decays to the states build in these minima have no gain in energy and, thus, less probable than the α decays to the states related to the ground state minima. The nucleus ^{259}No has only ground state potential minimum.

Figure 15 presents the energies of one-quasiparticle states build in the ground state potential minima. The values of Q_α for the ground-state-to-ground-state α decays are listed in Fig. 15 as well. Possible α decays are indicated in Fig. 15 and Table III. Even-odd heavy nuclei mainly decay by α to the states with the same spin and parity in the daughter nuclei. Within the accuracy of our calculations the calculated energies of α decays are close to those in Refs. [5,6].

Because in ^{271}Hs the state $3/2^+[611]$ is found to be above the states $9/2^+[615]$ and $11/2^-[725]$, it can be an isomeric state. The α decay from this state is possible to the same state in ^{267}Sg with $Q_\alpha = 9.12$ MeV. If the states $3/2^-[761]$ and $3/2^+[611]$ in ^{271}Hs would be above the $1/2^-[761]$ state, the last can be the isomer from which the α decay is possible with $Q_\alpha = 9.42$ MeV. The states $1/2^-[761]$ and $7/2^+[613]$ are related to the isomeric states in ^{267}Sg and ^{263}Rf, respectively. In ^{263}Rf, other isomer is the $11/2^-[725]$ state. The ground state of ^{263}Rf is found to be $1/2^-[761]$. Therefore, the spontaneous

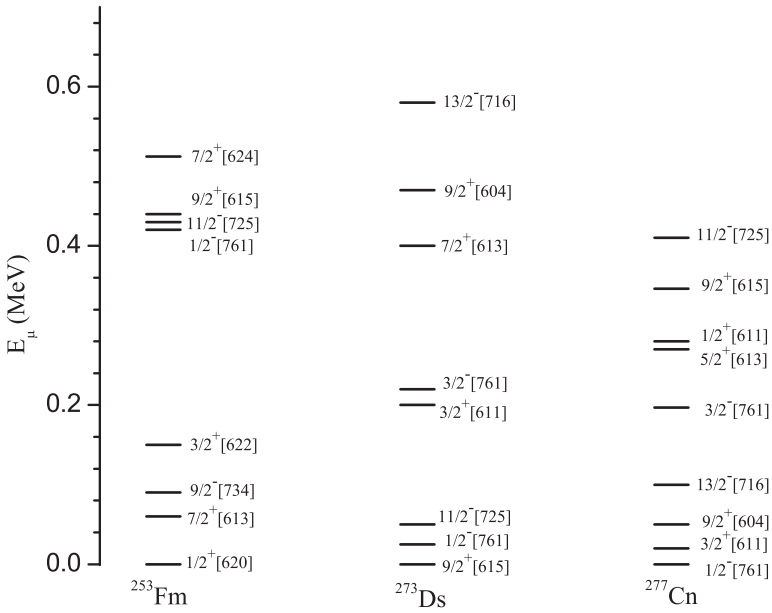

FIG. 11. The calculated spectra of one-quasineutron states in the nuclei ^{253}Fm, ^{273}Ds, and ^{277}Cn.

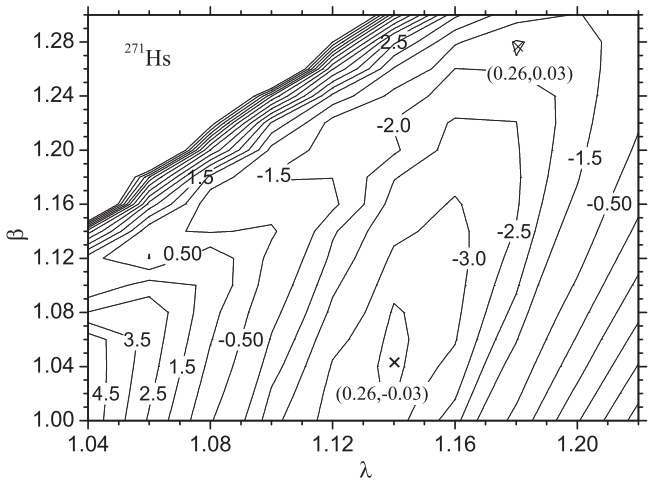

FIG. 12. The same as in Fig. 4, but for ^{271}Hs.

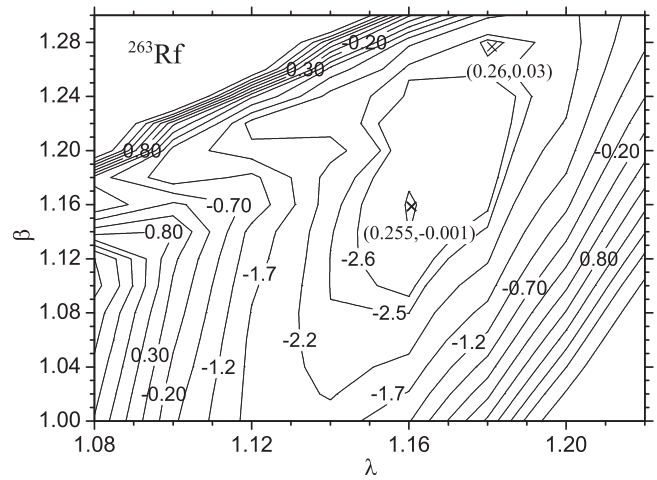

FIG. 14. The same as in Fig. 4, but for ^{263}Rf.

fission from the low-spin ground state of this even-odd nucleus can easily occur.

3. α-decay chain containing ^{270}Hs

Let us now consider the even-even nuclei in the α-decay chain: $^{270}\mathrm{Hs} \rightarrow {}^{266}\mathrm{Sg} \rightarrow {}^{262}\mathrm{Rf}$. In Fig. 16, the energies of two-quasiparticle states are presented with respect to the corresponding ground states. The calculated values of Q_α for the ground-state-to-ground-state α decays are shown and are in a good agreement with available experimental data. With $Q_\alpha \approx 9.2$ MeV in ^{270}Hs and Eq. (3) we obtain $T_\alpha \approx 6.4$ s. In the region of heaviest nuclei, the known K isomeric states live shorter time. Therefore, the α decays from the K isomers of ^{270}Hs seem to be improbable but can not be completely excluded based on our present knowledge. The possible transitions $^{270}\mathrm{Hs}(10^+_\pi) \xrightarrow{\alpha} {}^{266}\mathrm{Sg}(7^-_\pi) \xrightarrow{\alpha} {}^{262}\mathrm{Rf}(7^-_\pi \text{ or } 5^-_\pi)$ between the isomeric states would have $Q_\alpha = 9.55$ and 8.32 or 8.34 MeV that fits well the chain 14 in Ref. [5] ascribed to ^{271}Hs. The structures of these isomeric states are the following $10^+_\pi(9/2^+[624] \otimes 11/2^+[615])$, $7^-_\pi(5/2^-[512] \otimes 9/2^+[624])$, and $5^-_\pi(9/2^+[624] \otimes 1/2^-[521])$. The α decay of the ground state of ^{266}Sg with $Q_\alpha = 8.56$ MeV would need about 122 s that is too long in comparison with the spontaneous fission half-life 360 ms [6]. Note that the earlier data on the α-decay chains containing ^{266}Sg were reexamined in Ref. [52].

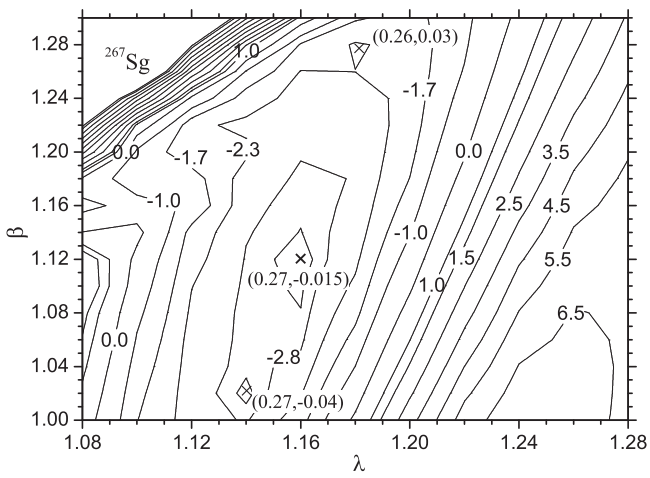

FIG. 13. The same as in Fig. 4, but for ^{267}Sg.

4. α-decay chain containing ^{268}Hs

For ^{272}Ds, ^{268}Hs, ^{264}Sg, ^{260}Rf, and ^{256}No, the calculated values of Q_α for the ground-state-to-ground-state α decays and the lowest two-quasiparticle states are presented in Fig. 17. In this α-decay chain the additional shallow potential minima exist in ^{268}Hs (at 0.12 MeV) and in ^{264}Sg (at 0.084 MeV). Other nuclei have only the ground-state potential minima. Using the Weisskopf estimate and taking into account the selection rules for the asymptotic quantum numbers, in ^{272}Ds the half-life time of isomeric state $6^+_\nu(11/2^-[725] \otimes 1/2^-[761])$ with respect to $E1$ transition into the state $5^-_\nu(9/2^+[604] \otimes 1/2^-[761])$ is 0.17 ms that is about 3 times shorter than the half-life time of this state with respect to the α decays into the isomeric state 6^+_ν or into the rotation state $6^+_{\mathrm{g.s.}}$ of ^{266}Hs. The α decay from the isomeric state 5^-_ν of ^{272}Ds into the rotational state $5^-_{\mathrm{g.s.}}$ of ^{268}Hs with $Q_\alpha = 11.44$ MeV and $T_\alpha \approx 5.5$ ms can occur if this isomeric state lives longer with respect to the γ decay. Note that the energies of the rotational states are calculated as in Ref. [49]. The reactions $^{240}\mathrm{Pu}(^{36}\mathrm{S},4n)^{272}\mathrm{Ds}$ [57] and $^{249}\mathrm{Cf}(^{22}\mathrm{Ne},3n)^{268}\mathrm{Hs}$ seem to be suitable for producing ^{272}Ds and ^{268}Hs, respectively.

In ^{268}Hs, the α decay from the isomer state 6^+_ν into the rotation state $6^+_{\mathrm{g.s.}}$ of ^{264}Sg can occur with $Q_\alpha = 10.66$ MeV and $T_\alpha \approx 81$ ms if this isomeric state does not decay by γs in a shorter time. Because the α decay from the isomeric state $10^-_\nu(11/2^-[725] \otimes 9/2^+[604])$ is estimated to need a long time $T_\alpha \approx 32$ s, this state would mainly decay by γs.

In ^{264}Sg, the α decays from the isomeric state $5^-_\pi(9/2^+[624] \otimes 1/2^-[521])$ into 5^-_π and $5^-_{\mathrm{g.s.}}$ states of ^{260}Rf demand at least 4.75 and 22 s, respectively, that is too long and the γ emission or fission from the isomeric state seem to be preferable. Analogously to ^{250}No [58], where the lowest 6^+_ν isomer is expected, the fission from K-isomer state can be

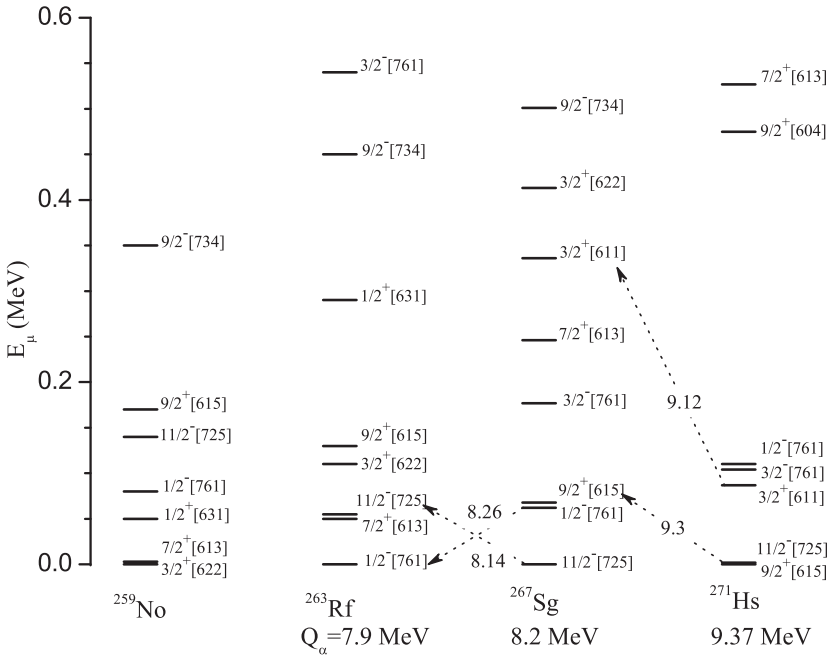

FIG. 15. The calculated spectra of one-quasineutron states in the indicated nuclei. For the ground-state-to-ground-state α decays, the calculated values of Q_α are presented. Possible α decays are shown by arrows with corresponding values of Q_α.

suppressed by about factor of 10. Larger spontaneous fission half-lives from the K isomers are supported by the calculations in Refs. [59,60]. Therefore, the spontaneous fission of ^{264}Sg in the event number 7 in Ref. [61] with relatively long lifetime can be related to the fission from the isomeric state 5^-_π.

In ^{260}Rf, the α decay from the isomer $5^+_\nu(7/2^+[613] \otimes 3/2^+[622])$ needs a rather long time. Therefore, the fission from this isomer would competes with its decay through the cascade of γ quanta. From the isomers $4^+_\nu(1/2^+[620] \otimes 7/2^+[613])$ and $8^-_\nu(7/2^-[514] \otimes 9/2^+[624])$ in ^{256}No both α decay and spontaneous fission seem to be longer than the decay through the cascade of γ quanta to the ground state.

IV. SUMMARY

The production of isotopes $^{268-271}$Hs was considered in various asymmetric reactions. The reactions resulting in larger yields of Hs isotopes are indicated. The calculated evaporation residue cross sections are in a good agreement with existing experimental data. This verifies our description of fusion at the bombarding energies near the Coulomb barrier taking into consideration the orientation effects.

The properties of several nuclei from the α-decay chains containing the isotopes $^{268-271}$Hs were investigated. The calculated energies of α decays are in satisfactory agreement with the available experimental data. For even-odd nuclei ^{253}Fm, ^{257,259}No, ^{261,263}Rf, ^{265,267}Sg, ^{269,271}Hs, ^{273}Ds, and ^{277}Cn, the calculated one-quasineutron spectra were presented and possible isomeric states were predicted. In the nuclei ^{269}Hs and ^{271}Hs the lowest K isomers are the states $1/2^-[761]$ at $E_\mu \approx 25$ keV and $3/2^+[611]$ at $E_\mu \approx 90$ keV, respectively. One cannot exclude the α decay and spontaneous fission, due to the small hindrance in K, from the isomer state $1/2^-_1[761]$ of ^{261}Rf.

The presence of isomeric states in several nuclei considered is expected. In the even-even heavy nuclei ^{252}Fm, ^{256}No, ^{260,262}Rf, ^{264,266}Sg, ^{268,270}Hs, and ^{272}Ds, the two-quasiparticle states and α decays from them were treated. In the nuclei ^{268}Hs and ^{270}Hs the lowest K-isomers are the states 6^+_ν, 10^-_ν at $E_\mu \approx 1.3$ MeV and 5^-_ν, 10^-_ν at $E_\mu \approx 1.1$ MeV, respectively. The α decays of isomeric state can be observed if the value of T_α is less than lifetime of K isomer with respect to the γ emission. The transitions $^{270}\text{Hs}(10^+_\pi) \xrightarrow{\alpha} {}^{266}\text{Sg}(7^-_\pi) \xrightarrow{\alpha} {}^{262}\text{Rf}(7^-_\pi \text{ or } 5^-_\pi)$ between the isomeric states fit well the chain 14 in Ref. [5] ascribed to ^{271}Hs. The spontaneous fission of ^{264}Sg in the

TABLE III. Possible α decays of indicated heavy nuclei starting from ^{271}Hs. The calculated values of Q_α and T_α, and tentatively related experimental values Q^{exp}_α of Q_α are listed.

Nucleus	Decay mode	Q_α (MeV)	T_α	Q^{exp}_α (MeV)
^{271}Hs	$9/2^+[615] \xrightarrow{\alpha} 9/2^+[615] \xrightarrow{\gamma} 11/2^-[725]$	9.3	3.24 s	9.27, 9.44 [5,6]
	$3/2^+[611] \xrightarrow{\alpha} 3/2^+[611] \xrightarrow{\gamma} 1/2^-[761], 11/2^-[725]$	9.12	11 s	
^{267}Sg	$11/2^-[725] \xrightarrow{\alpha} 11/2^-[725] \xrightarrow{\gamma} 7/2^+[613]$	8.145	2950 s	8.32 [6]
	$1/2^-[761] \xrightarrow{\alpha} 1/2^-[761]$	8.26	1225 s	
^{263}Rf	$1/2^-[761] \xrightarrow{\alpha} 1/2^-[761] \xrightarrow{\gamma} 3/2^+[622]$	7.8	9045 s	
	$7/2^+[613] \xrightarrow{\alpha} 7/2^+[613] \xrightarrow{\gamma} 3/2^+[622]$	7.87	5027 s	

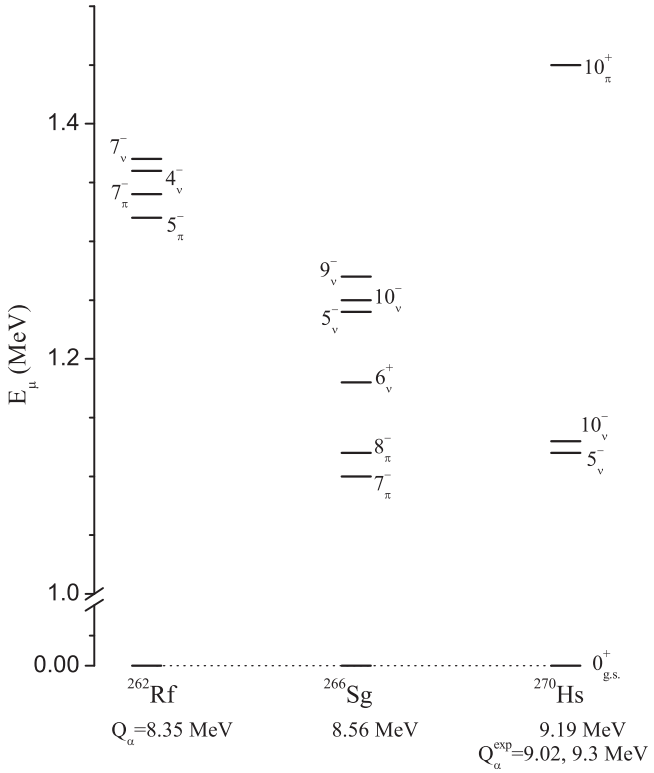

FIG. 16. The calculated energies E_μ of low-lying two-quasiparticle states in the indicated nuclei of the α-decay chain of ^{270}Hs. The calculated values of Q_α are compared with available experimental $Q_\alpha^{\rm exp}$ [5,6].

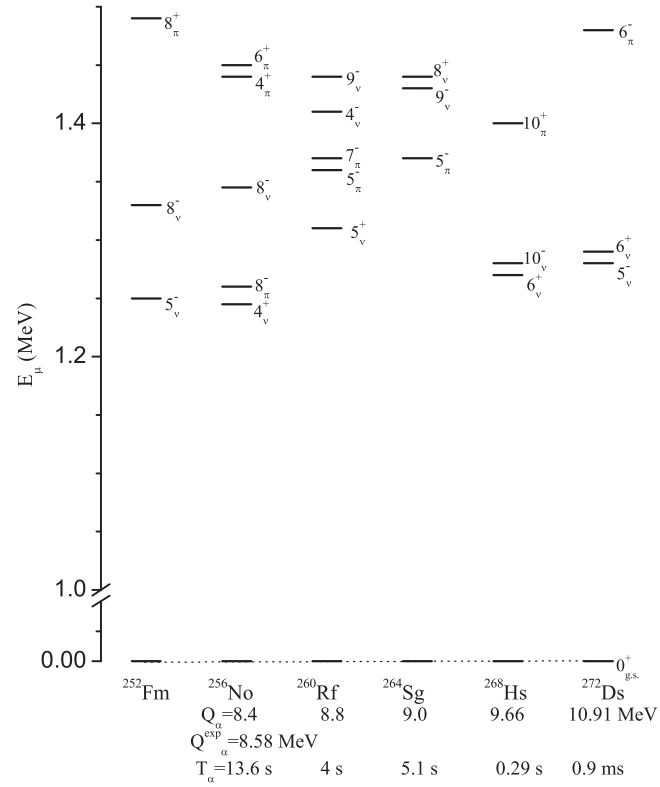

FIG. 17. The same as in Fig. 16, but for the nuclei of the α-decay chain containing ^{268}Hs. The calculated values of T_α are listed. The experimental values $Q_\alpha^{\rm exp}$ of Q_α are from Ref. [47].

event number 7 in Ref. [61] with relatively long lifetime one can relate to the fission from the isomeric state 5^-_π.

Besides the ground-state minima, the additional shallow minima were found on the potential energy surface of the nuclei $^{268-271}$Hs, $^{264-267}$Sg, and ^{261,263}Rf. Because these minima correspond to the deformation parameters close to those for the ground states, one can say that they are the shape isomers at the normal deformation. Because these additional minima are shallow, the nucleus can not be kept in them long enough to observe the γ transitions. However, the additional potential minima near the ground state can give evidence only in the α decays of heavy nuclei. The α decays can populate these minima in the daughter nucleus if they are quite close in energy to the ground state. The good candidate is the α decay of ^{265}Sg. Present experimental information is not sufficient to conclude whether the additional shallow potential minima found in a few nuclei have physical meaning. The appreciably larger pairing strength would wash out these minima. So, more data should be available to make a definite conclusion about the role of additional shallow minima near the ground state minimum.

ACKNOWLEDGMENTS

This work was supported in part by DFG-RFBR (Contract No. Le439/6-1). Polish-JINR (Dubna) Cooperation Programmes are gratefully acknowledged. The work of N.V.A. was partly supported by Tomsk Polytechnic University Competitiveness Enhancement Program grant.

[1] S. Hofmann and G. Münzenberg, Rev. Mod. Phys. **72**, 733 (2000).
[2] Yu. Oganessian, J. Phys. G **34**, R165 (2007).
[3] Y. A. Lazarev, Y. V. Lobanov, Y. T. Oganessian, V. K. Utyonkov, F. Sh. Abdullin, A. N. Polyakov, J. Rigol, I. V. Shirokovsky, Y. S. Tsyganov, S. Iliev, V. G. Subbotin, A. M. Sukhov, G. V. Buklanov, B. N. Gikal, V. B. Kutner, A. N. Mezentsev, K. Subotic, J. F. Wild, R. W. Lougheed, and K. J. Moody, Phys. Rev. C **54**, 620 (1996).
[4] S. Hofmann *et al.*, Eur. Phys. J. A **14**, 147 (2002).
[5] J. Dvorak, W. Brüchle, M. Chelnokov, R. Dressler, C. E. Düllmann, K. Eberhardt, V. Gorshkov, E. Jäger, R. Krücken, A. Kuznetsov, Y. Nagame, F. Nebel, Z. Novackova, Z. Qin, M. Schädel, B. Schausten, E. Schimpf, A. Semchenkov, P. Thörle, A. Turler, M. Wegrzecki, B. Wierczinski, A. Yakushev, and A. Yeremin, Phys. Rev. Lett. **97**, 242501 (2006).
[6] J. Dvorak, W. Brüchle, M. Chelnokov, C. E. Dullmann, Z. Dvorakova, K. Eberhardt, R. Eichler, E. Jäger, R. Krücken, A. Kuznetsov, Y. Nagame, F. Nebel, K. Nishio, R. Perego, Z. Qin, M. Schädel, B. Schausten, E. Schimpf, R. Schuber,

A. Semchenkov, P. Thörle, A. Türler, M. Wegrzecki, B. Wierczinski, A. Yakushev, and A. Yeremin, Phys. Rev. Lett. **100**, 132503 (2008).
[7] P. Möller and J. R. Nix, J. Phys. G **20**, 1681 (1994).
[8] Z. Patyk and A. Sobiczewski, Nucl. Phys. A **533**, 132 (1991).
[9] R. Smolanczuk, J. Skalski, and A. Sobiczewski, Phys. Rev. C **52**, 1871 (1995).
[10] V. V. Volkov, Izv. Akad. Nauk SSSR, Ser. Fiz. **50**, 1879 (1986); N. V. Antonenko, E. A. Cherepanov, A. K. Nasirov, V. B. Permjakov, and V. V. Volkov, Phys. Lett. B **319**, 425 (1993); Phys. Rev. C **51**, 2635 (1995).
[11] G. G. Adamian, N. V. Antonenko, S. P. Ivanova, and W. Scheid, Nucl. Phys. A **646**, 29 (1999).
[12] G. G. Adamian, N. V. Antonenko, W. Scheid, and V. V. Volkov, Nucl. Phys. A **633**, 409 (1998); Nuovo Cimento A **110**, 1143 (1997).
[13] G. G. Adamian, N. V. Antonenko, and W. Scheid, Nucl. Phys. A **678**, 24 (2000).
[14] A. S. Zubov, G. G. Adamian, N. V. Antonenko, S. P. Ivanova, and W. Scheid, Phys. Rev. C **68**, 014616 (2003).
[15] G. G. Adamian, N. V. Antonenko, and W. Scheid, Phys. Rev. C **69**, 011601(R) (2004); **69**, 014607 (2004); **69**, 044601 (2004).
[16] G. G. Adamian, N. V. Antonenko, and W. Scheid, in *Clustering Effects within the Dinuclear Model*, edited by Christian Beck, G. G. Adamian, N. V. Antonenko, and W. Scheid [Lect. Notes Phys., **848**, 165 (2012)].
[17] G. G. Giardina, S. Hofmann, A. I. Muminov, and A. K. Nasirov, Eur. Phys. J. A **8**, 205 (2000); G. G. Giardina, F. Hanappe, A. I. Muminov, A. K. Nasirov, and L. Stuttgé, Nucl. Phys. A **671**, 165 (2000); A. K. Nasirov *et al.*, *ibid.* **759**, 342 (2005); H. Q. Zhang, C. L. Zhang, C. J. Lin, Z. H. Liu, F. Yang, A. K. Nasirov, G. Mandaglio, M. Manganaro, and G. Giardina, Phys. Rev. C **81**, 034611 (2010); A. K. Nasirov, G. Mandaglio, G. G. Giardina, A. Sobiczewski, and A. I. Muminov, *ibid.* **84**, 044612 (2011).
[18] Z. H. Liu and J. D. Bao, Phys. Rev. C **74**, 057602 (2006).
[19] N. Wang, J. Tian, and W. Scheid, Phys. Rev. C **84**, 061601(R) (2011).
[20] N. Wang, E. G. Zhao, W. Scheid, and S. G. Zhou, Phys. Rev. C **85**, 041601(R) (2012); N. Wang, E. G. Zhao, and W. Scheid, *ibid.* **89**, 037601 (2014).
[21] L. Zhu, Z. Q. Feng, C. Li, and F. S. Zhang, Phys. Rev. C **90**, 014612 (2014); Z. Q. Feng, G. M. Jin, J. Q. Li, and W. Scheid, *ibid.* **76**, 044606 (2007).
[22] J. Hong, G. G. Adamian, and N. V. Antonenko, Phys. Rev. C **92**, 014617 (2015).
[23] X. J. Bao, Y. Gao, J. Q. Li, and H. F. Zhang, Phys. Rev. C **93**, 044615 (2016).
[24] J. Hong, G. G. Adamian, and N. V. Antonenko, Phys. Rev. C **94**, 044606 (2016); Phys. Lett. B **764**, 42 (2017); Phys. Rev. C **96**, 014609 (2017).
[25] S. Raman, C. W. Nestor, and P. Tikkanen, At. Data Nucl. Data Tables **78**, 1 (2001).
[26] K. H. Schmidt and W. Morawek, Rep. Prog. Phys. **54**, 949 (1991); K. H. Schmidt *et al.*, in *Proceedings of the Symposium on Physics and Chemistry of Fission*, Jülich (IAEA, Vienna, 1980), p. 409.
[27] G. G. Adamian, N. V. Antonenko, S. P. Ivanova, and W. Scheid, Phys. Rev. C **62**, 064303 (2000).
[28] A. S. Zubov, G. G. Adamian, N. V. Antonenko, S. P. Ivanova, and W. Scheid, Phys. Rev. C **65**, 024308 (2002).
[29] C.-C. Sahm *et al.*, Nucl. Phys. A **441**, 316 (1985).
[30] E. A. Cherepanov, A. S. Iljinov, and M. V. Mebel, J. Phys. G **9**, 931 (1983).
[31] R. Vandenbosch and J. R. Huizenga, *Nuclear Fission* (Academic Press, New York, 1973).
[32] A. V. Ignatyuk, K. K. Istekov, and G. N. Smirenkin, Sov. J. Nucl. Phys. **29**, 875 (1975).
[33] A. S. Iljinov *et al.*, Nucl. Phys. A **543**, 517 (1992).
[34] P. Möller, J. R. Nix, W. D. Myers, and W. J. Swiatecki, At. Data Nucl. Data Tables **59**, 185 (1995).
[35] R. Graeger, D. Ackermann, M. Chelnokov, V. Chepigin, C. E. Dullmann, J. Dvorak, J. Even, A. Gorshkov, F. P. Hessberger, D. Hild, A. Hubner, E. Jager, J. Khuyagbaatar, B. Kindler, J. V. Kratz, J. Krier, A. Kuznetsov, B. Lommel, K. Nishio, H. Nitsche, J. P. Omtvedt, O. Petrushkin, D. Rudolph, J. Runke, F. Samadani, M. Schadel, B. Schausten, A. Turler, A. Yakushev, and Q. Zhi, Phys. Rev. C **81**, 061601(R) (2010).
[36] Y. T. Oganessian, V. K. Utyonkov, F. S. Abdullin, S. N. Dmitriev, R. Graeger, R. A. Henderson, M. G. Itkis, Y. V. Lobanov, A. N. Mezentsev, K. J. Moody, S. L. Nelson, A. N. Polyakov, M. A. Ryabinin, R. N. Sagaidak, D. A. Shaughnessy, I. V. Shirokovsky, M. A. Stoyer, N. J. Stoyer, V. G. Subbotin, K. Subotic, A. M. Sukhov, Y. S. Tsyganov, A. Turler, A. A. Voinov, G. K. Vostokin, P. A. Wilk, and A. Yakushev, Phys. Rev. C **87**, 034605 (2013).
[37] A. Parkhomenko and A. Sobiczewski, Acta Phys. Pol. B **36**, 3115 (2005).
[38] Z. Lojewski, V. V. Pashkevich, and S. Cwiok, Nucl. Phys. A **436**, 499 (1985).
[39] S. G. Nilsson, C. F. Tsang, A. Sobiczewski, Z. Szymanski, S. Wycech, C. Gustafson, I.-L. Lamm, P. Möller, and B. Nilsson, Nucl. Phys. A **131**, 1 (1969).
[40] V. G. Soloviev, *Theory of Complex Nuclei* (Pergamon Press, Oxford, 1976).
[41] S. P. Ivanova, A. L. Komov, L. A. Malov, and V. G. Soloviev, Part. Nucl. **7**, 450 (1976).
[42] J. Maruhn and W. Greiner, Z. Phys. A **251**, 431 (1972).
[43] H. F. Zhang, Y. Gao, N. Wang, J. Q. Li, E. G. Zhao, and G. Royer, Phys. Rev. C **85**, 014325 (2012).
[44] G. G. Adamian, N. V. Antonenko, and W. Scheid, Phys. Rev. C **81**, 024320 (2010); G. G. Adamian, N. V. Antonenko, S. N. Kuklin, and W. Scheid, *ibid.* **82**, 054304 (2010); G. G. Adamian, N. V. Antonenko, S. N. Kuklin, B. N. Lu, L. A. Malov, and S. G. Zhou, *ibid.* **84**, 024324 (2011).
[45] A. N. Kuzmina, G. G. Adamian, and N. V. Antonenko, Eur. Phys. J. A **47**, 145 (2011); A. N. Kuzmina, G. G. Adamian, N. V. Antonenko, and W. Scheid, Phys. Rev. C **85**, 014319 (2012).
[46] A. Parkhomenko and A. Sobiczewski, Acta Phys. Pol. B **36**, 3095 (2005).
[47] http://www.nndc.bnl.gov/ensdf/.
[48] F. P. Hessberger, Eur. Phys. J. D **45**, 33 (2007).
[49] T. M. Shneidman, G. G. Adamian, N. V. Antonenko, and R. V. Jolos, Phys. Rev. C **74**, 034316 (2006).
[50] P. Möller, A. J. Sierk, T. Ichikawa, A. Iwamoto, R. Bengtsson, H. Uhrenholt, and S. Åberg, Phys. Rev. C **79**, 064304 (2009).
[51] J. Meng, J. Peng, S. Q. Zhang, and S.-G. Zhou, Phys. Rev. C **73**, 037303 (2006); J. Peng, H. Sagawa, S. Q. Zhang, J. M. Yao, Y. Zhang, and J. Meng, *ibid.* **77**, 024309 (2009); J. J. Li, W. H. Long, J. Margueron, and N. Van Giai, Phys. Lett. B **732**, 169 (2014).
[52] Ch. E. Düllmann and A. Türler, Phys. Rev. C **77**, 064320 (2008).

[53] N. V. Antonenko and L. A. Malov, Izv. RAN, Ser. Physics **78**, 1402 (2014).
[54] R. V. Jolos, L. A. Malov, N. Yu. Shirikova, and A. V. Sushkov, J. Phys. G **38**, 115103 (2011).
[55] K. Morita *et al.*, J. Phys. Soc. Jpn. **76**, 043201 (2007).
[56] M. Asai, K. Tsukada, M. Sakama, S. Ichikawa, T. Ishii, Y. Nagame, I. Nishinaka, K. Akiyama, A. Osa, Y. Oura, K. Sueki, and M. Shibata, Phys. Rev. Lett. **95**, 102502 (2005).
[57] J. Hong, G. G. Adamian, and N. V. Antonenko, Eur. Phys. J. A **52**, 305 (2016).
[58] D. Peterson, B. B. Back, R. V. F. Janssens, T. L. Khoo, C. J. Lister, D. Seweryniak, I. Ahmad, M. P. Carpenter, C. N. Davids, A. A. Hecht, C. L. Jiang, T. Lauritsen, X. Wang, S. Zhu, F. G. Kondev, A. Heinz, J. Qian, R. Winkler, P. Chowdhury, S. K. Tandel, and U. S. Tandel, Phys. Rev. C **74**, 014316 (2006).
[59] F. R. Xu, E. G. Zhao, R. Wyss, and P. M. Walker, Phys. Rev. Lett. **92**, 252501 (2004).
[60] H. L. Liu, F. R. Xu, Y. Sun, P. M. Walker, and R. Wyss, Eur. Phys. J. A **47**, 135 (2011); P. M. Walker, Nucl. Phys. A **834**, 22 (2010).
[61] K. Nishio *et al.*, Eur. Phys. J. A **29**, 281 (2006).